IIETA International Information and Engineering Technology Association
Advancing the World of Information and Engineering

Mathematical Modelling of Engineering Problems
Vol. 13, No. 4, April, 2026, pp. 751-766
Journal homepage: http://iieta.org/journals/mmep

Expanded Polystyrene-Modified Lightweight Concrete for Thermally Improved Rural Housing in High-Andean Regions

Caceres Bustamante Frank Whesler, Peralta Sánchez Luis Fernando, Yvan Huaricallo*

Faculty of Engineering, Private University of the North, Lima 07011, Peru

Corresponding Author Email: yvan.huaricallo@upn.pe

https://doi.org/10.18280/mmep.130412

Received: 1 August 2025
Revised: 20 November 2025
Accepted: 28 November 2025
Available online: 15 May 2026

Keywords:
expanded polystyrene, lightweight concrete, fine aggregate replacement, compressive strength, flexural strength, thermal performance, rural housing, high-Andean regions

ABSTRACT

This study investigates the feasibility of using expanded polystyrene (EPS) beads as a partial replacement for fine aggregate in lightweight concrete intended for rural housing in high-Andean regions. Four concrete mixtures containing 0%, 4%, 6%, and 8% EPS were designed with a target compressive strength of 21 MPa and evaluated in terms of workability, compressive strength, flexural strength, and residual performance after exposure to 1000 ℃. In addition, a full-scale housing prototype built with 4% EPS concrete blocks was assessed and compared with a conventional dwelling to examine its effect on indoor thermal conditions. The results indicate that the incorporation of EPS led to only minor reductions in compressive strength (1.69%–1.96%) and a more noticeable decrease in flexural strength (up to 18.68%); however, the mechanical performance remained within the acceptable range specified by the relevant testing standards. After high-temperature exposure, the concrete preserved approximately 94% of its initial compressive strength. The thermal assessment further showed that the EPS-based housing prototype achieved higher indoor temperatures than both the outdoor environment and the conventional dwelling, with improvements of 26% and 6%, respectively. Among the mixtures tested, the 4% EPS dosage provided the most appropriate balance between mechanical performance and thermal improvement. These findings indicate that EPS-modified lightweight concrete is a technically viable material for rural housing applications in cold high-altitude areas.

1. INTRODUCTION

The high Andean regions of Peru face severe climatic conditions, especially during frosty seasons, when temperatures can drop below 0 ℃. This situation, intensified by global climate change and the increase in atmospheric CO_2, has led to numerous cases of acute respiratory illnesses and premature deaths, primarily affecting children and the elderly [1]. In July 2010, the El Niño phenomenon caused a wave of extreme cold in South America, resulting in at least 45 deaths in the Peruvian highlands due to respiratory infections. In areas such as the Peruvian–Bolivian highlands, these events are recurrent and are aggravated by the thermal deficiencies of homes traditionally built with adobe or rammed earth [2-4]. Although these materials are accessible and inexpensive, their limited thermal insulation capacity poses a risk to the health and quality of life of residents. In this context, concrete construction represents a viable alternative because of its availability and strength. However, conventional concrete has high thermal conductivity, making it inefficient in cold climates unless technically modified with insulating materials.

To address this problem, recent studies have explored the incorporation of lightweight and thermally efficient materials, such as expanded polystyrene (EPS) beads, in concrete mixtures. EPS beads are thermoplastic polymers with a closed-cell structure containing up to 98% air, which significantly reduces heat transfer and decreases density while maintaining adequate strength [5, 6]. In Russia, EPS concretes have achieved compressive strengths between 0.28 and 4.22 MPa and thermal conductivities as low as 0.073 W/(m·℃), demonstrating strong potential for insulation applications [7-10]. In Latin America, studies in Colombia have combined Building Information Modeling (BIM) with phase-change materials (PCMs) to improve thermal comfort, while in Mexico, mortars combining limestone and recycled waste such as rubber and PET have been developed to balance thermal and mechanical performance [11, 12].

In Peru, national research has also produced encouraging results. In Macusani, for example, a classroom equipped with bioclimatic technology reached an indoor temperature of 13.36 ℃ compared to 6.60 ℃ in a conventional classroom, significantly improving comfort levels [13]. In Abancay, an insulating mortar incorporating wheat straw and cork raised the interior temperature by up to 4.5 ℃ without compromising mechanical strength (2.56–9.07 MPa) [14–16]. Other experiences in Chachapoyas proposed Styrofoam and plant-based mattresses to enhance adobe insulation, while in Tacna, adding EPS and rubber powder improved thermal efficiency without affecting structural integrity up to 10% inclusion [17-20].

Despite these advances, gaps remain in the literature. There is limited research on EPS-modified concretes simultaneously evaluated under real thermal conditions and controlled mechanical testing. Few studies have built full-scale housing prototypes to correlate indoor thermal performance with compressive and flexural strength, and replicable methodologies for Andean regions are scarce.

Accordingly, this study proposes a comprehensive experimental evaluation of concrete incorporating EPS beads at 4%, 6%, and 8% replacement levels. The analysis focuses on compressive and flexural behavior, fire resistance under exposure to 1000 °C, and the thermal comfort of a prototype dwelling constructed in the high-altitude district of Calquis, Cajamarca. Laboratory tests were performed following ASTM and Peruvian Technical Standards, while on-site monitoring compared the thermal behavior of an EPS-based dwelling with a conventional one. This integrated approach addresses the identified research gaps by: (i) combining structural and thermal analysis within a unified experimental design, (ii) constructing and monitoring a real-scale module in high Andean conditions, and (iii) documenting replicable construction processes for similar contexts.

The outcomes of this research directly contribute to the Sustainable Development Goals (SDGs): SDG 3 (Good Health and Well-Being), by mitigating cold-related illnesses; SDG 9 (Industry, Innovation, and Infrastructure), by promoting the use of innovative, low-cost materials; and SDG 11 (Sustainable Cities and Communities), by advancing resilient, affordable housing for vulnerable Andean populations. Its replicability is reinforced through standardized mix designs, compliance with national regulations, and field validation, providing technical evidence for future guidelines, local codes, and sustainable social housing programs in cold-climate regions of Peru.

2. METHODOLOGY

2.1 Type of research

This study adopts a quantitative experimental approach, based on the collection and statistical analysis of numerical data to test hypotheses about the effect of EPS inclusion on the physical and thermal properties of concrete [10]. The research is applied in nature, as it seeks to develop a replicable technical solution to a real habitability problem in the high-Andean regions of Peru.

The experimental design is completely randomized, incorporating a single independent variable, the percentage of EPS replacement (0%, 4%, 6%, and 8%), and several dependent variables, including compressive strength (f'_c), flexural strength (f'_r), thermal performance in the dwelling, and resistance of concrete exposed to 1000 °C. The design and statistical structure follow the methodological guidelines reported in previous studies [21-23]. Each treatment level was tested in triplicate to ensure experimental reliability and to allow subsequent analysis of variance (ANOVA) for determining significant differences among mixtures.

2.2 Population and sample

The population consisted of all test units produced in the laboratory: cylindrical specimens for compression, prismatic beams for flexural testing, and additional samples for thermal and fire resistance evaluations. At the field scale, a pilot housing module was constructed using EPS-modified concrete blocks, while a traditional dwelling served as a control model for comparative thermal monitoring.

The sample comprised 96 test specimens, distributed as shown in Table 1, and produced according to the ACI 211 mix design method [24, 25]. All mixtures were proportioned for a target compressive strength of 21 MPa using river aggregates and PERLA ETSAPOL EPS beads (density ≈ 10 kg/m³, size 3–7 mm). The number of specimens per mix and test type was determined to guarantee representativeness and consistency in mechanical and thermal performance assessment, ensuring compliance with ASTM C39 and Peruvian Technical Standards (NTP) 339.034.

Table 1. Total number of samples to be tested

Test Type / Curing Age	EPS 0%	EPS 4%	EPS 6%	EPS 8%	Subtotal
Compressive strength, 7 days	3	3	3	3	12
Compressive strength, 14 days	3	3	3	3	12
Compressive strength, 28 days	3	3	3	3	12
Flexural strength, 7 days	2	2	2	2	8
Flexural strength, 14 days	2	2	2	2	8
Flexural strength, 28 days	2	2	2	2	8
Residual compressive strength after exposure to 1000 °C, 7 days	3	3	3	3	12
Residual compressive strength after exposure to 1000 °C, 14 days	3	3	3	3	12
Residual compressive strength after exposure to 1000 °C, 28 days	3	3	3	3	12
Total	**24**	**24**	**24**	**24**	**96**

Note: EPS: expanded polystyrene; Total: 96 samples + construction of the experimental housing module.

Table 1 summarizes the number of specimens prepared for each test. Four concrete mixtures were evaluated: a reference mixture without EPS and three EPS-modified mixtures containing 4%, 6%, and 8% EPS beads. For each mixture, three cylindrical specimens were tested for compressive strength at curing ages of 7, 14, and 28 days. Three additional cylindrical specimens per mixture and curing age were exposed to 1000 °C to evaluate residual compressive strength. For flexural strength, two beam specimens were tested for each mixture at each curing age. In total, 96 specimens were prepared, excluding the experimental housing module.

2.3 Data collection techniques and instruments

The following techniques were used: (i) Structured observation, as a basic technique for process control, complying with what was suggested by Siddique et al. [13]. (ii) Content analysis, based on technical documents such as the National Building Regulations and standards such as ACI 211,

ASTM C39, and NTP 339.034 [26]. (iii) Technical instrumentation, using standardized equipment to perform slump tests (SLUMP, ASTM C143), compression, bending, humidity, absorption, and interior temperature monitoring (NTP 399.014:2014).

2.4 Experimental procedure

In this research, the effect of partially replacing fine aggregate with EPS beads was experimentally analyzed to evaluate its influence on the compressive and flexural strength of concrete, as well as on the thermal comfort of a prototype dwelling. Three EPS replacement levels—4%, 6%, and 8%—were tested for the mechanical properties, and the mixture that most closely matched the standard concrete performance was selected for the thermal evaluation phase.

All laboratory tests were carried out at the Universidad Privada del Norte (UPN) under controlled conditions, following ASTM and NTP applicable to the evaluation of concrete materials. The procedures complied with ASTM C39 / NTP 339.034 for compressive strength, ASTM C78 / NTP 339.078 for flexural strength, and NTP 399.014:2014 for thermal performance monitoring.

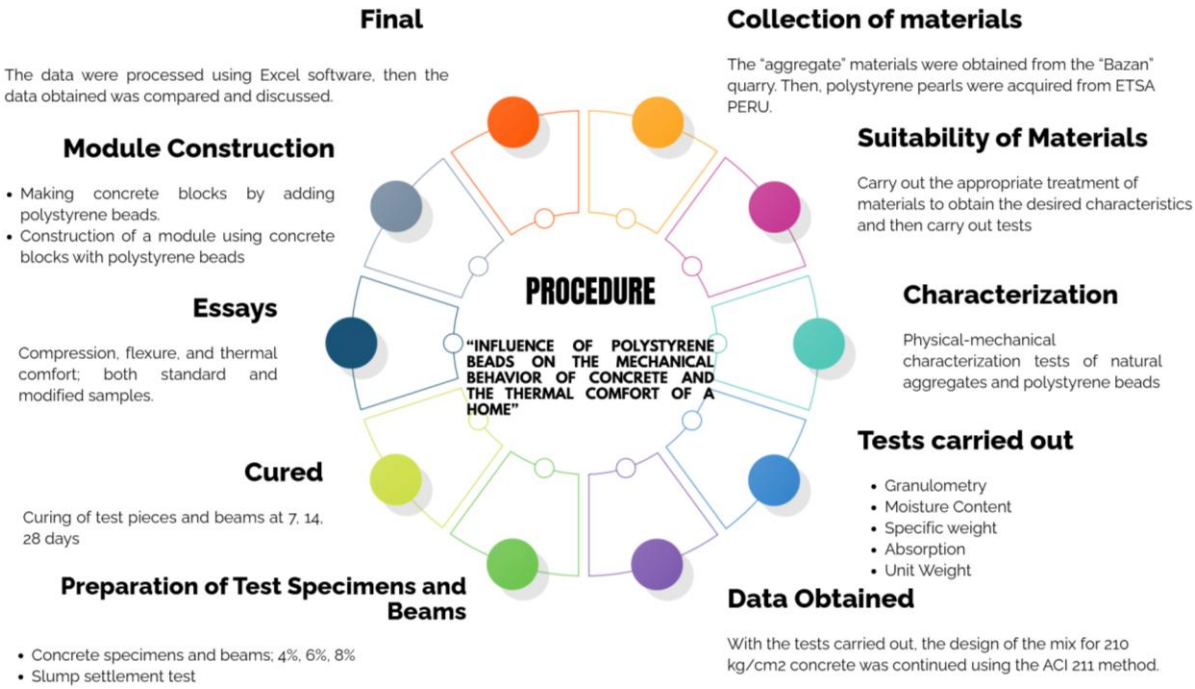

Figure 1. Procedure outline
Note: Diagram for the research development process.

Figure 2. Location of Bazán quarry
Note: Map of the location of the Bazán quarry (Source: Google Earth).

The experimental program was structured in sequential stages: (i) selection and characterization of materials; (ii) mix design and specimen preparation; (iii) mechanical testing at curing ages of 7, 14, and 28 days; (iv) exposure of samples to 1000 °C to evaluate fire resistance; and (v) construction and thermal monitoring of a full-scale housing module. The general workflow of these procedures is illustrated in Figure 1.

2.5 Aggregate collection

For this research, the "Bazán" quarry was selected to obtain the necessary aggregates for this study, using river materials to achieve greater strength. Figure 2 shows that the quarry is located 50 m from Huambocancha Baja, in Cajamarca, specifically at kilometer 3 of the Cajamarca Highway leading to Bambamarca.

Collection of materials:

- Natural aggregates from the Bazán quarry (Cajamarca), selected for their controlled granulometry [15].
- PERLA ETSAPOL brand EPS, 10 kg/m³ and 3–7 mm in size, purchased from ETSA Peru.
- Aggregate characterization: Granulometric analysis (ASTM C136 / NTP 400.012), humidity and absorption (ASTM C127, C128 / NTP 400.021), unit weight (ASTM C29 / NTP 400.017).
- Design and preparation of mixtures: Four designs (0%, 4%, 6%, 8% EPS) for f'_c = 21 MPa.
- ACI Method 211 [12]. Slump test according to ASTM C143 / MTC E705.

2.6 Preparation of specimens

Concrete specimens were prepared according to standardized procedures. Cylindrical samples were produced to determine the f'_c following ASTM C39 / NTP 339.034, while rectangular beams were fabricated for the modulus of rupture (M_r), also referred to as flexural strength test in accordance with ASTM C78 / NTP 339.078. All samples were cast using the four mix designs (0%, 4%, 6%, and 8% EPS), compacted in two layers, and cured under controlled humidity and temperature until the designated testing ages of 7, 14, and 28 days.

2.7 Exposure to high temperature

To assess the fire resistance of the concrete, additional specimens from each mix were subjected to 1000 °C following the ISO 834 standard fire curve [16]. The exposure was carried out in a controlled furnace for one hour, and post-exposure compressive strength tests were performed to evaluate the residual capacity and integrity of the EPS-modified concrete.

2.8 Construction of the experimental housing module

A full-scale prototype housing module was built using concrete blocks containing 4% EPS, selected based on optimal mechanical and thermal performance. The module measured 3 m × 5 m, with a reinforced concrete foundation designed in accordance with RNE E.050. The roof was constructed with galvanized tin sheets compliant with NTP 399.010-009, and the structure was equipped with thermal instrumentation following NTP 399.014:2014 to monitor indoor temperature variations.

2.9 Thermal monitoring and comparison

Temperature data were recorded hourly in three settings: the EPS-based module, a conventional dwelling built with traditional materials, and the outdoor environment. Measurements were carried out during both summer and rainy seasons to capture the thermal behavior under different climatic conditions.

2.10 Data processing and analysis

All experimental data were processed using descriptive statistics, including mean values and standard deviations, to ensure the reliability and consistency of the results. Comparative analyses were conducted to evaluate percentage variations in mechanical strength, residual strength after exposure to 1000 °C, and thermal performance among the different EPS dosages and in comparison with the reference concrete mixture. In addition, ANOVA and complementary statistical tests were applied to identify significant differences between the experimental groups.

2.11 Ethical aspects

The research complied with the ethical standards stipulated in the National Building Regulations and ISO 9001, ensuring transparency, reproducibility, and respect for scientific integrity. All tests were conducted in accredited laboratories, with no manipulation of results.

2.12 Replicability of the study

This work employs standardized and regulated procedures, allowing for replicability in high Andean regions with similar conditions. The detailed documentation of design, execution, control, and evaluation provides a useful technical framework for engineers, public administrators, and social housing programs.

3. RESULTS

3.1 Physical tests

3.1.1 Particle size analysis

Summary tables of the physical and mechanical properties of the aggregates are presented, together with the results of axial compressive strength of cylindrical specimens, flexural strength of beam specimens, and compressive strength of cylindrical specimens after exposure to 1000 °C.

Table 2 indicates a continuous particle-size distribution for the fine aggregate, with the largest fractions retained between sieves No. 30 and No. 8, and only ≈ 1.77% passing the No. 200—which meets ASTM C33 limits. The cumulative percentages remain within the lower/upper limits prescribed by the standard across the sieve range.

Figure 3 graphically indicates the same result: the granulometric curve of the fine aggregate lies within the ASTM C33 envelope, showing a slight tendency toward a coarser grading.

The particle size distribution test of fine aggregates was performed in the university laboratory using sieves No. 4, 8,

16, 30, 50, 100, and 200, and the corresponding pans. The results obtained were as follows: the material retained most was obtained with sieve No. 30, the average particle size was 3/8 in., the fineness modulus was 2.82, and the particle size distribution curve is within the range allowed by the particle size distribution spindle. In conclusion, the tested material is suitable for further investigation, as shown in Table 2.

Figure 4 shows the particle size distribution results obtained for the coarse aggregate in the concrete laboratory of Universidad Privada del Norte. The granulometric analysis was performed using the following sieves: 1 1/2 in., 1 in., 3/4 in., 1/2 in., 3/8 in., No. 4, and pan. The highest retained percentage was observed in the 1/2 in. sieve. The maximum aggregate size was 1 1/2 in., the nominal maximum size was 3/4 in., and the fineness modulus was 2.09. The particle size distribution curve remained within the permissible grading limits, indicating that the coarse aggregate was suitable for the subsequent concrete mixture design and experimental testing.

Table 2. Fine aggregate (FA) particle size test

No.	Sieve		Retained Weight (gr)	Retained (%)	Accumulated Retained (%)	Granulometric Spindles (According to ASTM C33 Standard)	
	(in)	(mm)				Lower Limit	Upper Limit
1	No. 4	4.75	14.30	2.84	2.84	95	100
2	No. 8	2.36	75.70	15.01	17.85	80	100
3	No. 16	1.18	82.30	16.32	34.17	50	85
4	No. 30	0.60	120.00	23.80	57.97	25	60
5	No. 50	0.30	96.80	19.20	77.17	10	30
6	No. 100	0.15	74.00	14.68	91.85	2	10
7	No. 200	0.075	32.20	6.39	98.23	0	3
8	Tray	-	8.90	1.77	100.00	-	-

Note: This table shows the weights retained on sieves for the AF.

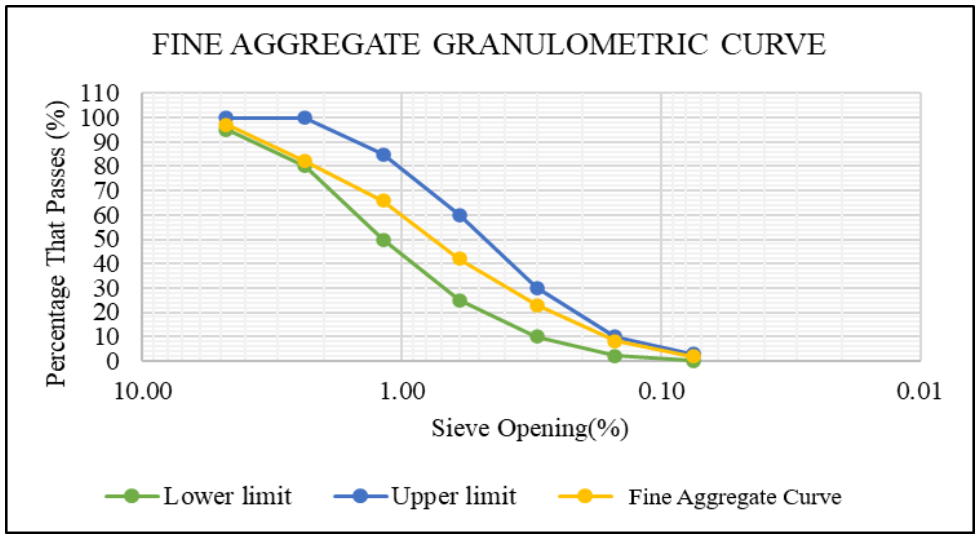

Figure 3. Curve of the granulometry of the fine aggregate (FA)
Note: This figure shows the weights retained on sieves for the FA.

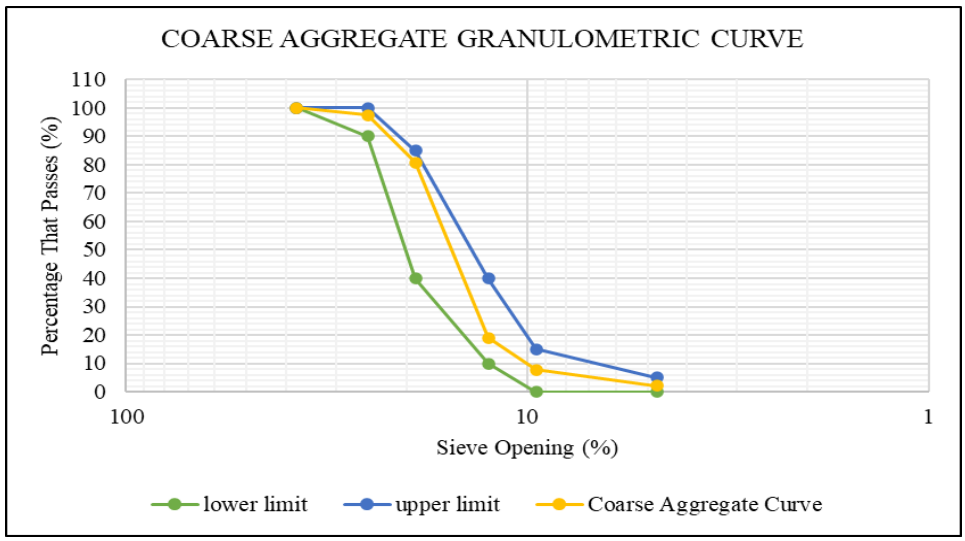

Figure 4. Granulometric curve of the coarse aggregate (CA)
Note: This figure shows the weights retained on each sieve for the CA.

Table 3. Moisture content of fine and coarse aggregates

Aggregate Moisture Content	
Fine aggregate	5.04%
Coarse aggregate	0.57%

Note: Values represent the average moisture content of the aggregates used in the mix design.

Table 3 shows the procedure and results of the test performed on the fine aggregate to obtain the moisture content of the fine and coarse aggregates. For this test, 3 samples of each of the aggregates were used to average the results and obtain more accurate data. The average moisture content of the fine aggregate was 5.04%, and the average moisture content of the coarse aggregate was 0.57%, results that will be used for the design of concrete in the different dosages.

3.1.2 Loose and compacted unit weight of fine aggregate

Table 4 presents the results and representative images from the tests conducted on fine aggregate to determine its loose and compacted unit weights. Three samples were used in this test, and the average values obtained are 1486.68 kg/m³ for the loose unit weight and 1593.27 kg/m³ for the compacted unit weight. These values are subsequently used in the design of concrete mixtures with different dosages.

Table 5 presents the results and representative images from the tests conducted on coarse aggregate to determine loose and compacted unit weights based on three samples. The average values obtained are 1456.39 kg/m³ for the loose unit weight and 1488.31 kg/m³ for the compacted unit weight. These values are subsequently used in the design of concrete mixtures with different dosages.

Table 4. Loose and compacted unit weight test of fine aggregate (FA)

Unit Weight of Fine Aggregate		
Description	**Loose Unit Weight (kg/m³)**	**Compacted Unit Weight (kg/m³)**
FA	1486.68	1593.27

Note: Values represent the loose and compacted unit weights of the fine aggregate.

Table 5. Loose and compacted unit weight test of coarse aggregate (CA)

Unit Weight of Coarse Aggregate		
Description	**Loose Unit Weight (kg/m³)**	**Compacted Unit Weight (kg/m³)**
CA	1456.39	1488.31

Note: This table shows the loose weight and the weight after the compaction process of the coarse aggregate.

3.1.3 Absorption and specific gravity

The results of the specific gravity and water absorption tests for fine aggregates, which are essential for mix design development, are presented in Table 6. The fine aggregate exhibits a specific gravity of 2.68 g/cm³ and a water absorption of 2.92%.

Table 6. Absorption and specific gravity test of fine aggregates (FAs)

Specific Gravity and Absorption of Fine Aggregate		
Description	**Specific Gravity (g/cm³)**	**Absorption (%)**
FA	2.68	2.92

Note: The table shows the specific gravity and absorption of the fine aggregate.

Table 7. Absorption and specific gravity test of coarse aggregates (CAs)

Specific Gravity and Absorption of Coarse Aggregate		
Description	**Specific Gravity(g/cm³)**	**Absorption (%)**
CA	2.59	1.15

Note: The table shows the specific weight and absorption of the aggregates.

Similarly, the results of the specific gravity and water absorption tests for coarse aggregates are shown in Table 7. The coarse aggregate has a specific gravity of 2.59 g/cm³ and a water absorption of 1.15%.

3.1.4 Workability

The slump test measures the workability of the concrete mix, which impacts how easily it can be molded into the formwork. Therefore, the slump in inches was determined for the four concrete mix designs.

Table 8 and Figure 5 show the influence that the different dosages of polystyrene pearls have on the composition of the concrete, where it is observed that the polystyrene pearls increase the slump value, but still maintain a plastic consistency in the mixture, which guarantees adequate workability.

Table 8. Workability test with different mix designs

Design	Response Time	Slump (cm)	Consistency
Pattern design	0'	09.57	Plastic
Design with 4% EPS	0'	09.25	Plastic
Design with 6% EPS	0'	09.85	Plastic
Design with 8% EPS	0'	10.05	Plastic

Note: This table shows the concrete slump value measured at zero time after mixing for each design.

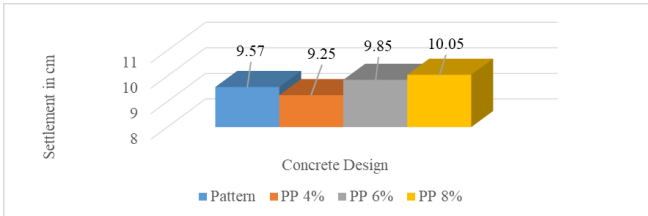

Figure 5. Workability of concrete mixtures with different EPS bead contents

Note: PP: Polystyrene Pearls; EPS: expanded polystyrene. The bar chart compares the slump values of the reference mixture and the EPS-modified concrete mixtures.

3.2 Mechanical tests

3.2.1 Compressive strength

Table 9, Figure 6, and Figure 7 show that the use of polystyrene beads in the composition of the concrete has a slight negative effect at all curing ages, moderately decreasing the f'_c value as the EPS content increases. The standard mix reached an average compressive strength of 301.56 kg/cm² (≈ 29.58 MPa) after 28 days of curing. The mixes with 4%, 6%, and 8% polystyrene beads reached average strengths of 296.45 kg/cm², 296.39 kg/cm², and 295.63 kg/cm², respectively, demonstrating only a minimal decrease in axial load capacity as the EPS dosage increased.

Although the target design strength was 21 MPa, the higher strength obtained in the control mix is fully consistent with the overdesign margin recommended by the ACI 211.1-91 method, which suggests an excess of approximately 25–35% to ensure that the specified strength is achieved under field

conditions. Since the specimens were produced and cured under controlled laboratory conditions with high-quality local aggregates and optimized water–cement ratio, it is technically reasonable that the resulting compressive strength exceeded the nominal design value. Therefore, this difference does not indicate an error in mix design or material control, but rather reflects the controlled environment and intrinsic quality of the materials used.

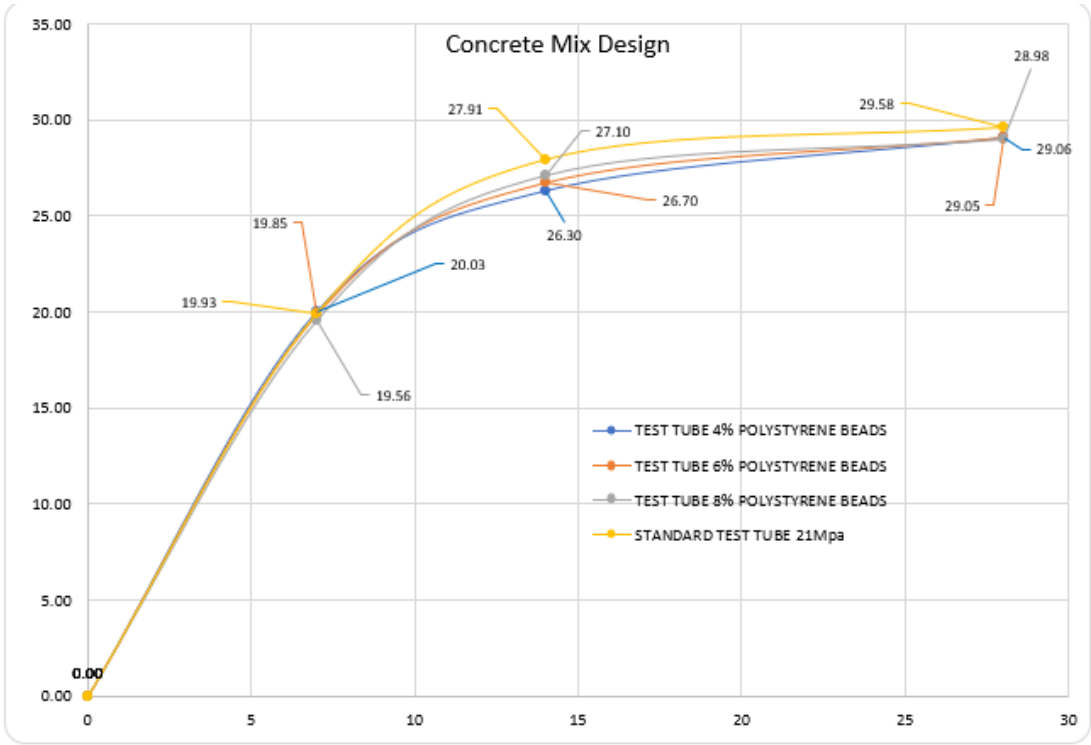

Figure 6. Comparative diagram of the f'_c curves of the concrete designs
Note: The graph shows the comparison of the compressive strength of concrete for its 4 designs.

Table 9. Summary of f'_c test of cylindrical samples of the standard concrete and with polystyrene beads at 4%, 6%, 8%

Design	Age	f'_c (MPa)	Standard Deviation
Pattern concrete	7	19.93	1.54
	14	27.91	3.12
	28	29.58	1.04
Concrete with 4% polystyrene beads	7	20.03	4.5
	14	26.30	4.78
	28	29.06	8.97
Concrete with 6% polystyrene beads	7	19.85	2.09
	14	26.70	3.87
	28	29.05	1.35
Concrete with 8% polystyrene beads	7	19.56	5.11
	14	27.10	3.14
	28	28.98	5.56

Note: This table shows the summary of f'_c of the concrete for the 4 designs and at curing ages of 7, 14, and 28 days.

Considering both the mechanical behavior and the fresh properties, the 4% EPS dosage was selected as the most suitable proportion for the construction of the prototype housing module in the district of Calquis.

The relatively high standard deviation (SD) observed in the 4% EPS mix (SD = 8.97 MPa) is attributed to the heterogeneous distribution of EPS beads within the cementitious matrix, which produces localized porosity and variable density. This variability is inherent to lightweight concretes containing polymeric inclusions and remains within the range reported by Siddique et al. [13]. Despite this dispersion, the ANOVA test indicated no statistically significant difference in compressive strength ($p > 0.6$).

Table 10. Summary of f'_c test of cylindrical specimens for the 4 designs subjected to 1000 °C

Design	Age	f'_c (MPa)	Standard Deviation
Pattern concrete	7	19.24	7
	14	24.81	4.13
	28	28.22	13.09
Concrete with 4% polystyrene beads	7	17.97	4.91
	14	24.63	7.25
	28	27.93	5.95
Concrete with 6% polystyrene beads	7	17.80	1.25
	14	24.40	10.60
	28	26.60	8.47
Concrete with 8% polystyrene beads	7	17.69	8.99
	14	23.76	10.40
	28	26.32	5.06

Note: The results show a reduction in compressive strength after exposure to 1000 1000 °C and curing ages of 7, 14, and 28 days. It can be seen that it negatively affects the concrete.

3.2.2 Compressive strength of specimens exposed to 1000 °C

Table 10 and Figures 8-10 present the results and their comparisons, showing that the incorporation of polystyrene beads into concrete exposed to 1000 °C led to a reduction in compressive strength compared with the reference concrete. After 28 days of curing, the reference sample at 0 °C reached an average compressive strength of 29.58 MPa, while the reference sample exposed to 1000 °C reached 28.22 MPa. The concrete mixtures containing 4%, 6%, and 8% polystyrene beads and exposed to 1000 °C achieved average compressive strengths of 27.93 MPa, 26.60 MPa, and 26.32 MPa, respectively, indicating a gradual reduction in resistance to axial loading. Exposure to 1000 °C produced a measurable

reduction in compressive strength, although the reduction was not statistically significant for the selected comparisons. Compared with the reference concrete at 0 °C, the strength decreased by 4.52% for the reference concrete exposed to 1000 °C, by 5.58% for the mixture containing 4% polystyrene beads, by 10.07% for the mixture containing 6% polystyrene beads, and by 11.02% for the mixture containing 8% polystyrene beads. The maximum reduction was therefore observed in the mixture with 8% polystyrene beads; however, all mixtures remained within the acceptable strength range. Based on these results, the selected percentages of polystyrene beads were considered suitable for the proposed concrete mixtures, although lower replacement levels showed better agreement with the reference design.

3.2.3 Flexural strength of beams

Table 11 and Figure 11 show the use of polystyrene beads in the composition of the concrete for the production of beams subjected to flexural testing. The standard sample reached an average value of 4.87 MPa after 28 days of curing. The mixtures contain the inclusion of 4% polystyrene beads, an average value of 4.50 MPa; with the equivalent addition of 6% polystyrene beads, a value of 4.07 MPa; and with the addition of 8% polystyrene beads, a value of 3.96 MPa, demonstrating a decrease in resistance to flexural loading loads. The design is considered acceptable at all addition percentages and remains within the required range; considering this, it was decided to add 4% polystyrene beads as it best fits the standard design.

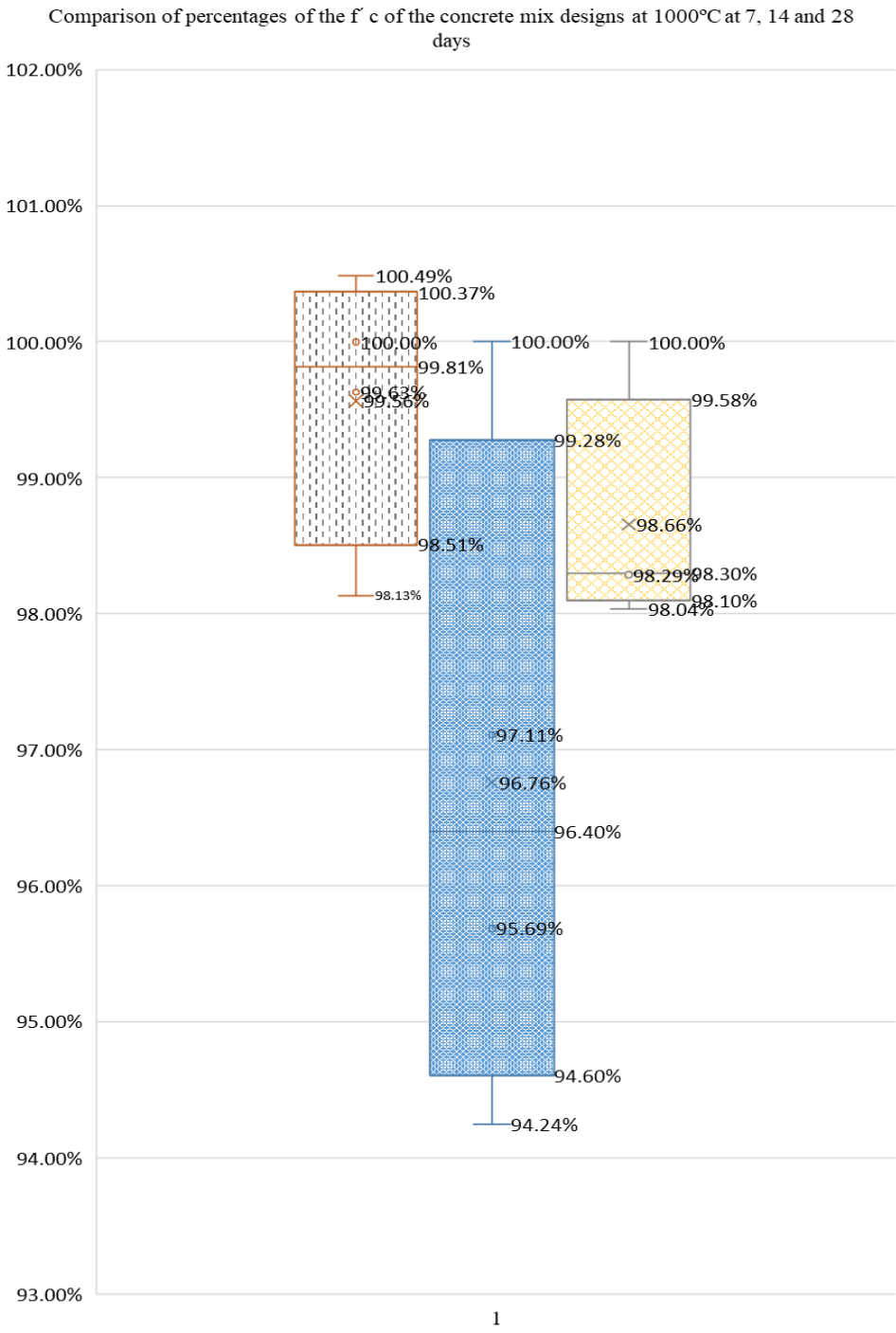

Figure 7. Comparative diagram of the average f'_c of the concrete designs

Note: The graph shows the comparison of the compressive strength of the concrete for its 4 designs at 7, 14, and 28 days, showing the maximum and minimum values.

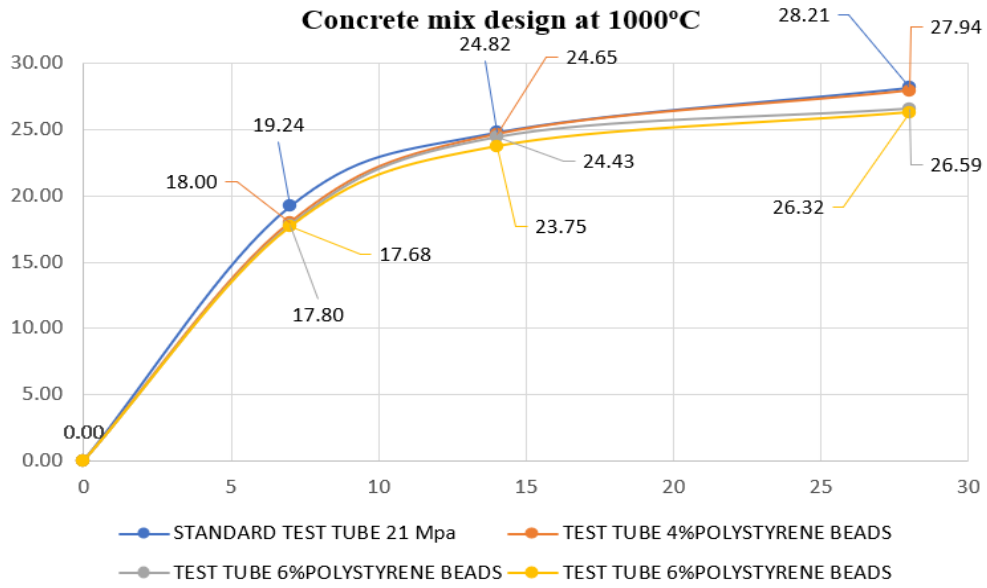

Figure 8. Comparative diagram of the f'_c curves of the concrete designs

Note: The graph shows the comparison of the compressive strength of concrete for its 4 designs that were subjected to 1000 °C of temperature.

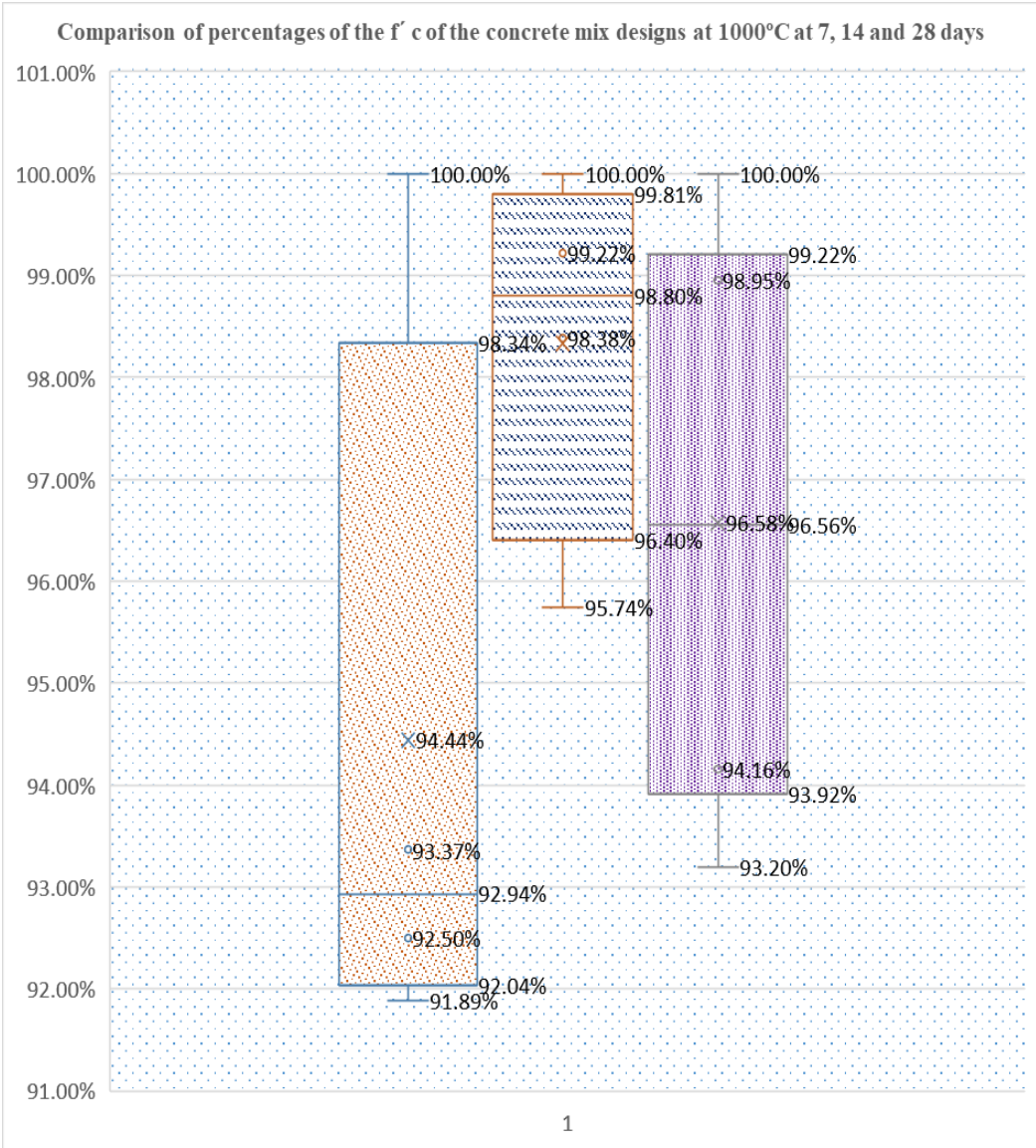

Figure 9. Comparative diagram of the average f'_c of concrete designs subjected to 1000 °C

Note: The graph shows the comparison of the compressive strength of concrete subjected to 1000 °C on its 4 designs at 7, 14, and 28 days, showing the maximum and minimum values.

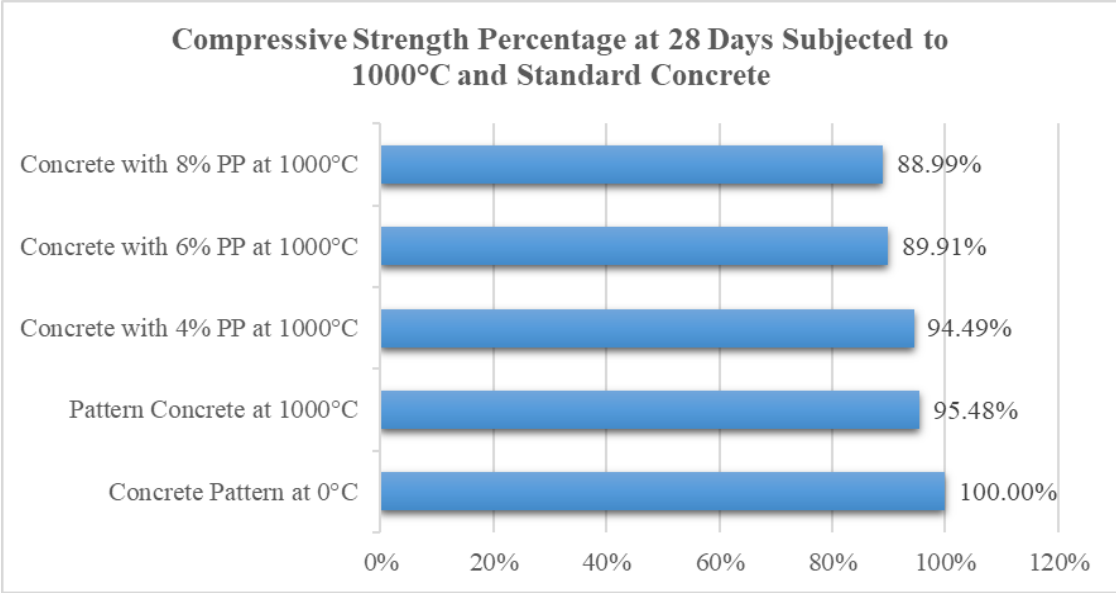

Figure 10. Comparative diagram in percentages of compressive strength subjected to 1000 °C
Note: The graph shows the compressive strength of the 4 designs subjected to 1000 °C, compared to the standard concrete at 0 °C.

Table 11. Summary of modulus of rupture (M_r) test of concrete with polystyrene beads at 4%, 6%, 8%

Design	Age	M_r (MPa)	Maximum Deflection (mm)
Pattern concrete	7	4.21	0.253
	14	4.54	0.292
	28	4.87	0.288
Concrete with 4% polystyrene beads	7	3.71	0.257
	14	4.11	0.262
	28	4.50	0.268
Concrete with 6% polystyrene beads	7	3.72	0.251
	14	3.72	0.263
	28	4.07	0.266
Concrete with 8% polystyrene beads	7	3.62	0.243
	14	3.76	0.255
	28	3.96	0.269

Note: This table shows M_r concrete's summary for the 4 designs and at curing ages of 7, 14, and 28 days.

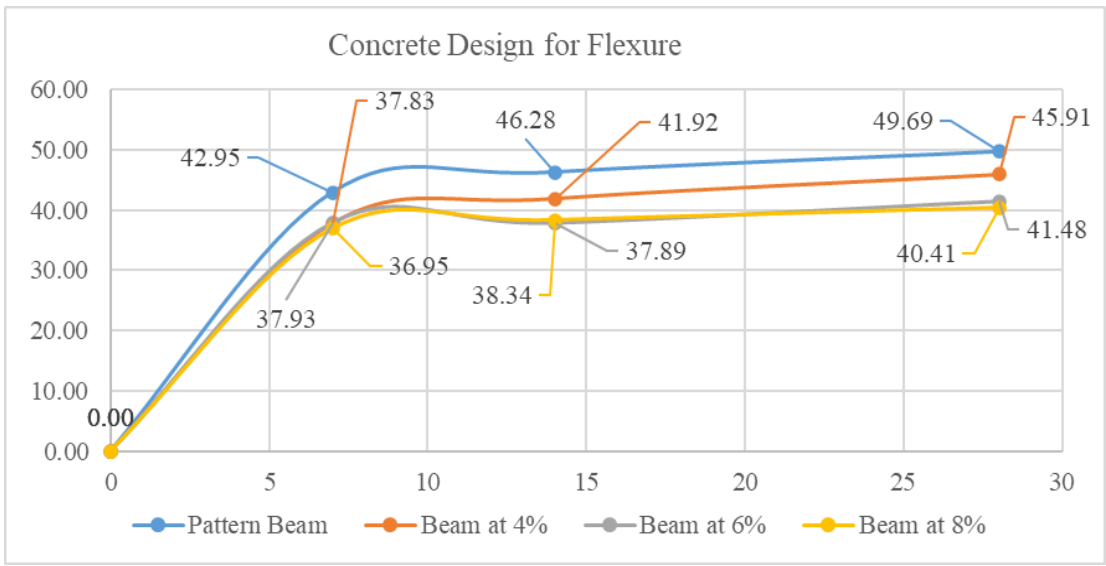

Figure 11. Comparative diagram of the modulus of rupture (M_r) curves of the concrete designs
Note: The graph shows the flexural modulus of rupture of the 4 designs.

3.3 Thermal comfort tests

Tables 12-13 and Figures 12-16 show the performance of the housing module constructed with 4% EPS beads in the district of Calquis, where thermal comfort was evaluated and compared with both a conventional module in the area and the outdoor ambient temperature at the different times of day. Measurements were taken during two distinct climatic

conditions:

During the summer season (08/11/2024), 17hourly samples were recorded between 05:00 and 20:00 h. The average outdoor temperature was 8.93 ℃, the conventional module reached 12.01 ℃, and the EPS-based module achieved 13.82 ℃. The relevant and consistent comparison—against the conventional module—indicates a +1.81 ℃ (≈ 15%) improvement in indoor temperature.

During the rainy season (10/01/2025), 17 samples were taken under similar conditions. The average outdoor temperature was 7.56 ℃, the conventional dwelling reached 9.89 ℃, and the EPS-based module achieved 12.41 ℃, showing a +2.52 ℃ (≈ 25%) increase compared with the conventional module.

These values were recalculated to ensure a consistent reference baseline, taking the conventional module as the control rather than the outdoor environment. The results indicate that the use of EPS significantly improves indoor thermal comfort under both seasonal conditions, with statistically significant gains ($p < 0.001$). The statistical results presented in Table 14 indicate that the inclusion of EPS as a fine aggregate replacement up to 8% did not produce statistically significant variations in the compressive strength of concrete at 28 days ($p > 0.6$). A one-way ANOVA test, rather than a Pearson correlation, was applied to compare the mean compressive strengths among the four EPS replacement levels (0%, 4%, 6%, 8%), because EPS content was treated as a categorical factor in this analysis. Where appropriate, Welch's t-test was further used for pairwise comparisons to account for possible unequal variances among groups. The ANOVA and Welch's t-test results show that the observed strength reductions, which were below 2%, fall within the expected variability of cement-based materials and can be explained by the relatively weak mechanical bonding at the EPS–cement interface.

However, the flexural strength showed a marginal reduction with borderline ($p \approx 0.05$), suggesting that the lower stiffness and smooth surface of EPS particles may create interfacial discontinuities that restrict tensile stress transfer and slightly weaken the bending capacity. These results indicate that, although EPS has a limited effect on tensile-related properties, it does not compromise compressive performance, which is the primary load-bearing criterion for non-structural concrete elements.

Table 12. Outdoor temperature samples taken from a conventional module and the module made with expanded polystyrene (EPS) concrete blocks on a clear day in Calquis

Date	Hour	Outdoor Environment (℃)	EPS-Based Module (℃)	Conventional Module (℃)
08/11/2024	00:00	6.90	10.70	8.90
08/11/2024	05:00	6.20	12.30	10.10
08/11/2024	06:00	7.90	13.50	10.80
08/11/2024	07:00	8.60	12.90	11.30
08/11/2024	08:00	9.05	13.00	11.30
08/11/2024	09:00	9.60	13.50	12.60
08/11/2024	10:00	10.20	14.30	12.10
08/11/2024	11:00	10.80	14.20	12.50
08/11/2024	12:00	11.50	15.50	13.00
08/11/2024	1:00 PM	10.40	14.70	12.20
08/11/2024	2:00 PM	10.15	15.10	13.50
08/11/2024	3:00 PM	9.80	14.30	12.40
08/11/2024	4:00 PM	7.60	13.80	12.30
08/11/2024	17:00	8.25	14.10	12.40
08/11/2024	18:00	8.30	14.30	12.48
08/11/2024	19:00	8.40	14.40	13.10
08/11/2024	8:00 PM	8.20	14.30	13.20

Note: This table shows the temperature summary in ℃ of the manufactured module in the Calquis district during the summer.

Table 13. Outdoor temperature samples taken in a conventional module and a module made with expanded polystyrene (EPS) concrete blocks during the rainy season in Calquis

Date	Hour	Outdoor Environment (℃)	EPS-Based Module (℃)	Conventional Module (℃)
10/01/2025	00:00	5.40	9.30	7.40
10/01/2025	05:00	5.00	11.20	8.90
10/01/2025	06:00	6.50	12.20	9.40
10/01/2025	07:00	7.00	11.40	9.70
10/01/2025	08:00	7.70	11.80	9.95
10/01/2025	09:00	8.50	12.50	11.50
10/01/2025	10:00	8.90	13.10	10.80
10/01/2025	11:00	9.40	12.90	11.10
10/01/2025	12:00	10.30	13.60	11.80
10/01/2025	1:00 PM	9.10	13.50	10.90
10/01/2025	2:00 PM	8.90	13.00	10.20
10/01/2025	3:00 PM	8.60	13.20	10.30
10/01/2025	4:00 PM	6.50	12.80	10.70
10/01/2025	17:00	6.95	12.90	9.30
10/01/2025	18:00	7.00	12.80	9.20
10/01/2025	19:00	7.00	12.10	9.10
10/01/2025	8:00 PM	5.80	12.60	7.90

Note: This table shows the temperature summary in ℃ of the manufactured module, in the Calquis district, on a rainy day.

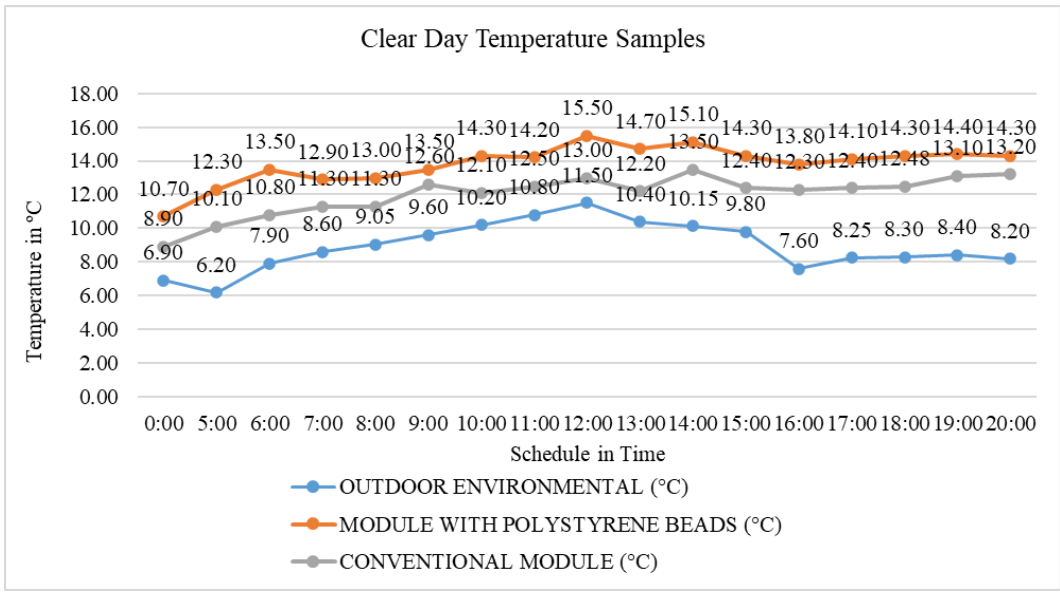

Figure 12. Comparative diagram of temperature curves at the different times of day during the summer season

Note: The graph shows the temperature difference between the modules and the outdoor environment of the Calquis – San Miguel – Cajamarca community, using the time series analysis method.

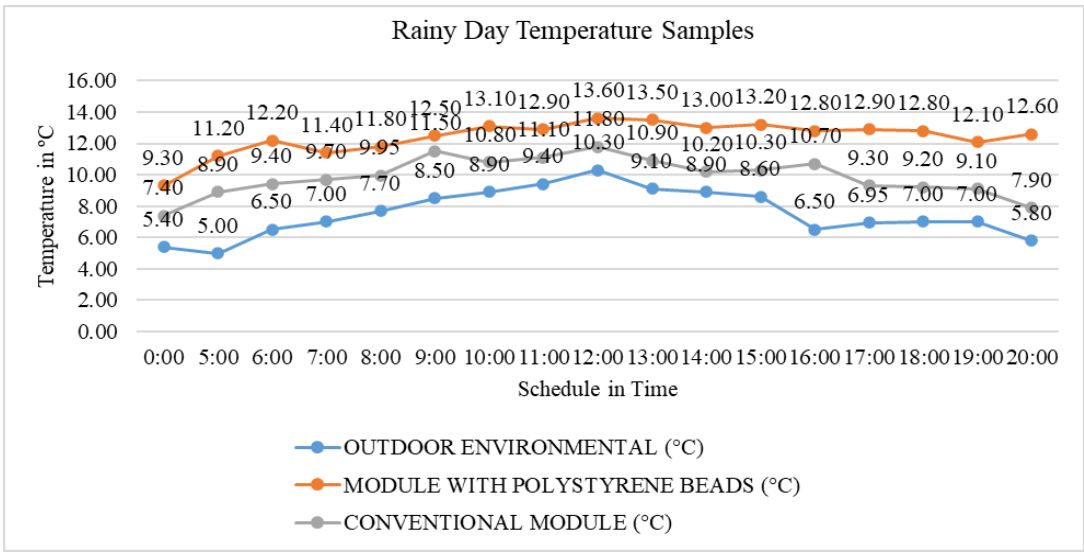

Figure 13. Comparative diagram of temperature curves at different times of a rainy season day

Note: The graph shows the temperature difference between the modules and the outdoor environment in the Calquis – San Miguel – Cajamarca community during the rainy season.

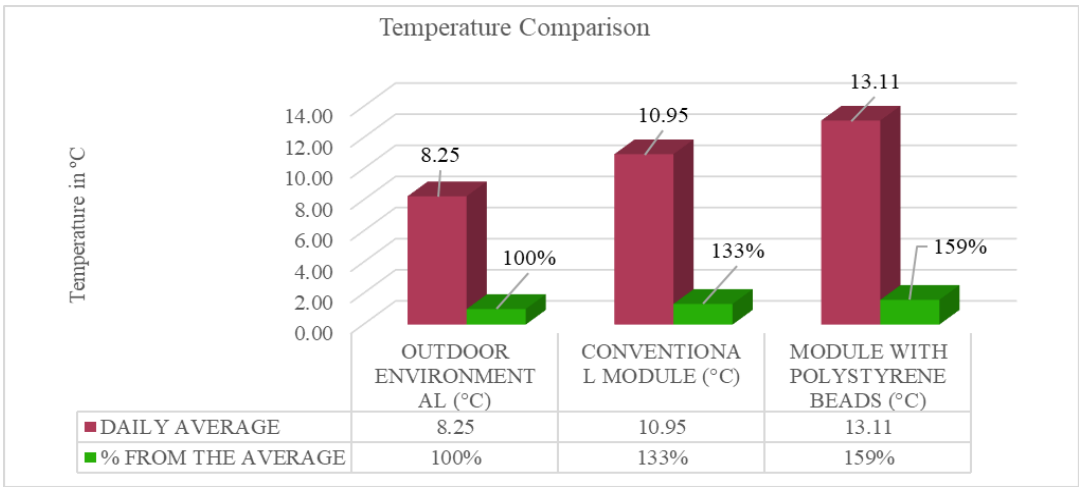

Figure 14. Comparative diagram of daily average and temperature percentages

Note: The graph shows the percentage difference between the average temperatures and the percentages of the modules compared.

Figure 15. Construction of the module
Note: 4% polystyrene beads.

Under high-temperature exposure at 1000 °C, the ANOVA results indicated no statistically significant reduction in compressive strength ($p > 0.6$), suggesting that the material maintained acceptable mechanical stability when EPS was incorporated at moderate dosages (≤ 4%). This behavior may be associated with the thermal response of EPS and the resulting pore structure after high-temperature exposure; however, the mechanism should be interpreted cautiously, as EPS can soften, melt, and decompose under elevated temperatures. The paired t-tests for the thermal performance data showed highly significant differences ($p < 0.001$), indicating that the observed indoor temperature improvements of +1.3 °C in summer and +2.4 °C during the rainy season were unlikely to result from random variations but represented measurable improvements in indoor thermal conditions. Thus, the data suggest a clear mechanical–thermal balance: EPS can improve thermal performance without statistically compromising compressive performance, provided that its dosage remains within the approximately 4% range.

Figure 16. Temperature taking
Note: The temperature reading is displayed on the block module, which includes 4% polystyrene beads.

Table 14. Statistical analysis of the mechanical and thermal behavior of expanded polystyrene-modified concrete

Property / Variable	Comparison	Mean ± Standard Deviation	Test Applied	P-Value	Statistical Significance	Interpretation
Compressive strength (28 d)	0% EPS vs. 4% EPS	29.58 ± 1.04 vs. 29.06 ± 8.97 MPa	One-way analysis of variance (ANOVA) / Welch's t-test	0.73	Not significant ($p > 0.05$)	An EPS ≤ 4% does not significantly affect compressive strength.
Compressive strength (28 d)	0% EPS vs. 8% EPS	29.58 ± 1.04 vs. 28.98 ± 5.56 MPa	ANOVA	0.67	Not significant	Strength reduction < 2%; within normal variability range.
Flexural strength (28 d)	0% EPS vs. 8% EPS	4.87 vs. 3.96 MPa	Welch's t-test	0.048	Marginally significant	Reduction in tensile transfer due to a weaker EPS–cement interface.
Residual strength (1000 °C)	0% EPS vs. 4% EPS	28.22 vs. 27.93 MPa	ANOVA	0.64	Not significant	EPS at low content retains ≈ 94% of initial compressive strength (f'_c); no structural failure.
Indoor temperature (summer)	EPS 4% vs. Conventional	13.9 °C vs. 12.6 °C	Paired t-test	< 0.001	Highly significant	EPS improves indoor temp by +1.3 °C; indicated statistical gain.
Indoor temperature (rainy)	EPS 4% vs. Conventional	12.5 °C vs. 10.1 °C	Paired t-test	< 0.001	Highly significant	The EPS module maintains +2.4 °C above control; enhanced comfort.

Table 15. Summary of statistical and technical effects

Effect	Statistical Result	Technical Interpretation
Mechanical effect	$p > 0.6$	No significant difference in compressive strength; expanded polystyrene (EPS) ≤ 4% is structurally acceptable.
Flexural effect	$p \approx 0.05$	Slightly significant reduction due to elastic mismatch at the EPS–cement interface.
Thermal effect	$p < 0.001$	Highly significant temperature gain indicates thermal insulation benefit.
Overall trade-off	Not applicable	EPS 4% achieves an optimal balance between strength retention and thermal efficiency.

In Table 15, the synthesis of results reinforces the dual behavior of EPS in concrete—mechanically neutral but thermally advantageous. The mechanical effects were statistically non-significant ($p > 0.6$), indicating that moderate EPS incorporation maintains the functional strength of the concrete matrix and complies with NTP 339.034 requirements. The flexural effect was marginally significant ($p \approx 0.05$), which aligns with theoretical predictions of reduced stress transmission through polymeric inclusions. On the other hand, the thermal effect exhibited strong statistical significance ($p < 0.001$), highlighting the capacity of EPS to act as a heat barrier by reducing conductive and convective heat flow through the concrete mass. Overall, the trade-off analysis indicates that the 4% EPS dosage achieves the optimal balance between structural reliability and thermal efficiency, representing a practical and statistically validated solution for high-Andean construction contexts.

This combined interpretation supports the selection of EPS concrete as a sustainable, low-cost material capable of mitigating heat loss in cold climates while maintaining acceptable mechanical behavior for non-structural or lightly loaded applications. The statistical validation strengthens the reliability of the findings, ensuring that the improvements in thermal performance are not anecdotal but quantitatively significant and replicable under similar environmental and experimental conditions.

4. DISCUSSION

The inclusion of EPS enhances thermal efficiency while slightly compromising mechanical strength. The reduction in strength can be attributed to weaker interfacial bonding and increased void content in the cementitious matrix. EPS's closed-cell structure reduces heat transfer, effectively improving thermal comfort. Trade-offs between EPS dosage, compressive strength, and thermal gain were identified, supporting 4% EPS as the most balanced composition.

4.1 Mechanical behavior of expanded polystyrene-modified concrete

The compressive strength results demonstrated a progressive decrease as EPS content increased. At 28 days, the standard concrete achieved 29.58 MPa, while mixtures with 4%, 6%, and 8% EPS reached 29.06 MPa, 29.05 MPa, and 28.98 MPa, respectively. The reduction trend agrees with the study [12], which reported that EPS particles form weak interfaces with the cementitious matrix due to their smooth, hydrophobic surface, reducing bonding efficiency while enhancing insulation. Nevertheless, the observed reduction of only 1.96% remains within the limits established by the Peruvian Technical Standard NTP 339.034, indicating that moderate EPS dosages (≤ 4%) do not compromise the structural integrity of low-load or non-structural elements.

In comparison, Siddique et al. [13] observed that replacing fine aggregate with 9% ground glass increased the compressive strength of concrete ($f'_c = 21$ MPa), emphasizing that the chemical reactivity and surface morphology of the substitute material determine its effect on strength. Unlike angular glass, which exhibits strong mechanical interlock and bond affinity, EPS is chemically inert and lacks surface roughness, explaining the mild reduction observed here.

Similarly, the M_r decreased with increasing EPS content, consistent with the theoretical model proposed by Yu et al. [14]. At 28 days, the flexural strength declined from 4.87 MPa in the control mixture to 4.50 MPa with 4% EPS and 3.96 MPa with 8%. This trend results from the lower stiffness of EPS particles and the formation of microvoids that interrupt the stress transfer path in the matrix. These findings suggest that EPS reduces tensile resistance more than compressive capacity, a conclusion consistent with composite material behavior in lightweight concretes.

4.2 Compressive strength at high temperatures

Concrete performance under 1000 °C exposure also showed strength loss, consistent with findings in the literature. The standard concrete exhibited a 4.52% reduction, while EPS mixtures decreased by 5.58% (4% EPS), 10.07% (6% EPS), and 11.02% (8% EPS). These results compare favorably with those of the study [15], which reported a 22.6% loss in conventional concrete under similar thermal exposure. The relatively small degradation observed here suggests that EPS, despite being thermoplastic, does not cause catastrophic failure when incorporated in controlled proportions. Instead, the residual compressive strength indicates that EPS partially melts and fills voids before volatilization, mitigating microcracking propagation. However, at higher dosages, thermal expansion and pore coalescence increase, compromising structural cohesion. Therefore, in fire-resistance applications or environments with potential high-temperature exposure, EPS incorporation should not exceed 4%.

4.3 Influence of expanded polystyrene on thermal comfort

The most notable outcome of this study is the improvement in thermal comfort within the EPS-based module. During the summer, the indoor temperature averaged 13.82 °C compared to 12.01 °C in the conventional module and 8.93 °C outdoors. In the rainy season, temperatures averaged 12.41 °C (EPS), 9.89 °C (conventional), and 7.56 °C (outdoors), representing a 26% improvement relative to the external environment and a 6% gain over traditional construction. These differences are statistically significant ($p < 0.001$) and support the insulating capacity of EPS concrete.

Such results align with Fang et al. [16], who observed a 6.76 °C thermal increase in Macusani using bioclimatic strategies, and with Liu and Jiang [17], who demonstrated that natural additives like straw and cork can raise indoor temperatures by up to 4.5 °C. In this study, the thermal gain is attributed to the closed-cell structure and 98% air content of EPS, which substantially lowers thermal conductivity [4]. Compared to organic additives and PCMs, EPS offers superior durability, easy mixing with traditional concrete, and greater long-term stability under variable humidity and radiation conditions (ambient temperature 18–20 °C, relative humidity (RH) 65–70%, solar radiation ≈ 820 W/m² during testing).

4.4 Critical synthesis

The results collectively indicate that the inclusion of 4% EPS provides the optimal balance between mechanical performance and thermal efficiency. Higher EPS dosages yield diminishing thermal returns while significantly reducing flexural resistance and residual strength at elevated temperatures. This equilibrium dosage (4%) thus represents a

practical threshold for sustainable, thermally efficient concrete suitable for high-Andean regions.

This research provides empirical validation under real-life mountain conditions, contributing to the design of sustainable construction materials aligned with SDG 3 (Good Health and Well-being), SDG 9 (Industry, Innovation and Infrastructure), and SDG 11 (Sustainable Cities and Communities). The findings strengthen the argument for using locally available EPS waste as a feasible substitute for fine aggregates, supporting circular economy practices and resilience in rural housing. The proposed framework can be adapted to other highland areas, promoting replicable, cost-effective, and environmentally responsible housing solutions in Peru and similar regions.

5. LIMITATIONS AND IMPLICATIONS

Despite the positive outcomes, this study has several limitations. The experiment was conducted in Calquis, Cajamarca, which restricts the generalization of the results to regions with different climatic and construction conditions. The housing module tested was small-scale; therefore, the structural and thermal behavior in larger or multi-story buildings remains to be validated.

Additionally, only one type of EPS was assessed, without considering variations in density or particle size, which may influence mechanical and thermal performance. The thermal evaluation was limited to the summer and rainy seasons and did not cover a full annual cycle, thereby constraining long-term performance assessment.

Furthermore, mechanical tests were conducted under controlled laboratory conditions rather than dynamic or seismic loading scenarios. Another limitation was the lack of a comparable housing structure with equivalent dimensions and materials in the study area, which prevented direct performance comparison.

Future research should focus on large-scale validation, long-term thermal monitoring, and the integration of digital modeling tools (e.g., BIM-based simulations) to improve the applicability and scalability of the findings.

6. CONCLUSIONS

The findings of this research demonstrate that incorporating EPS beads as a partial replacement for fine aggregate slightly decreases the mechanical strength of concrete but significantly enhances its thermal performance under high-Andean climatic conditions.

At 28 days, mixtures containing 4%, 6%, and 8% EPS reached compressive strengths of 29.06 MPa, 29.05 MPa, and 28.98 MPa, respectively—representing small reductions of –1.69%, –1.71%, and –1.96% compared to the control concrete (29.58 MPa). These variations indicate that moderate EPS dosages (≤ 4%) do not compromise the structural integrity of low-load or non-structural elements. Similarly, Mr showed a gradual decline, reaching 3.96 MPa at 8% EPS (–18.68%), which is attributed to the lower stiffness and weaker interfacial bond of EPS particles within the cement matrix.

Workability results indicated that all mixtures remained within the plastic consistency range, with only a slight reduction observed for the 4% EPS mix (9.25 cm) compared to the control (9.57 cm). Under thermal exposure at 1000 °C, compressive strength losses did not exceed –6.80%, and the 4% EPS design exhibited minimal deterioration (–1.05%). All residual values complied with the requirements of NTP 339.034, indicating adequate performance under fire conditions.

Thermal testing validated the working hypothesis: the housing module built with 4% EPS concrete blocks achieved an average indoor temperature of 13.78 °C during the rainy season—higher than both the conventional dwelling (11.23 °C) and the outdoor environment (9.63 °C). This represents a 26% improvement relative to external conditions and a 6% gain compared to traditional construction.

In summary, the controlled incorporation of EPS (up to 4%) provides an effective and sustainable strategy to improve indoor comfort in frost-prone Andean regions without significantly compromising mechanical behavior. The use of EPS-modified concrete thus constitutes a replicable, energy-efficient, and climate-adapted construction solution, promoting sustainable housing development and alignment with SDG 9 (Industry, Innovation, and Infrastructure) and SDG 11 (Sustainable Cities and Communities) in rural Andean communities.

REFERENCES

[1] Abdelkader, F., Naimi, O., Mohamed, R., Cheikh, K., Ahmed, Z., Sakhi, T., Roqiya, D., Mahieddine, C. (2024). The impact of fibres reinforcement on the thermal characteristics of lime-stabilised compressed earth blocks. Studies in Engineering and Exact Sciences, 5(1): 432-448. https://doi.org/10.54021/seesv5n1-026

[2] Waghe, U., Agrawal, D., Ansari, K., Wagh, M., Amran, M., Alsulami, B.T., Maqbool, H.M., Gamil, Y. (2024). Enhancing eco-concrete performance through synergistic integration of sugarcane, metakaolin, and crumb rubber: Experimental investigation and response surface optimization. Journal of Environmental Research, 12(4): 645-658. https://doi.org/10.1016/j.jer.2023.09.009

[3] Peralta, W.J.C., Vilca, Y.H., Flores, A.D.P. (2023). Improving thermal quality in rural housing using fiber cement blocks in Masocruz, Puno region. Ingeniería y Geología, 26(52): e25057. https://doi.org/10.15381/iigeo.v26i52.25057

[4] Malode, S.J., Shetti, N.P. (2025). Thermal energy storage systems using bio-based phase change materials: A comprehensive review for building energy efficiency. Journal of Energy Storage, 105: 114709. https://doi.org/10.1016/j.est.2024.114709

[5] Somani, P., Gaur, A. (2024). Thermo-mechanical analysis of microencapsulated phase change material incorporated in concrete pavement. Materials Letters, 366: 136520. https://doi.org/10.1016/j.matlet.2024.136520

[6] Almutairi, A.L., Tayeh, B.A., Adesina, A., Isleem, H.F., Zeyad, A.M. (2021). Potential applications of geopolymer concrete in construction: A review. Case Studies in Construction Materials, 15: e00733. https://doi.org/10.1016/j.cscm.2021.e00733

[7] Arslan, M., Ghaffar, E., Sohail, A., Pallonetto, F., Waseem, M. (2025). Comprehensive examination of thermal energy storage through advanced phase change material integration for optimized building energy

management and thermal comfort. Energy and Built Environment, 1(1). https://doi.org/10.1016/j.enbenv.2025.03.003
[8] Chen, J., Dan, H., Ding, Y., Gao, Y., et al. (2021). New innovations in pavement materials and engineering: A review on pavement engineering research 2021. Journal of Traffic and Transportation Engineering, 8(6): 815-999. https://doi.org/10.1016/j.jtte.2021.10.001
[9] Chen, L., Yang, M., Chen, Z., Xie, Z., et al. (2024). Conversion of waste into sustainable construction materials: A review of recent developments and prospects. Materials Today Sustainability, 27: 100930. https://doi.org/10.1016/j.mtsust.2024.100930
[10] Cong, P., Cheng, Y. (2021). Advances in geopolymer materials: A comprehensive review. Journal of Traffic and Transportation Engineering, 8(3): 283-314. https://doi.org/10.1016/j.jtte.2021.03.004
[11] Longo, F., Cascardi, A., Lassandro, P., Aiello, M.A. (2021). Energy and seismic drawbacks of masonry: A unified retrofitting solution. Journal of Building Pathology and Rehabilitation, 6(1): 31. https://doi.org/10.1007/s41024-021-00121-6
[12] Jaramillo, H.Y., Zuluaga-Gallego, R., Arango-Correa, A., García-León, R.A. (2025). Thermoacoustic, physical, and mechanical properties of bio-bricks from agricultural waste. Buildings, 15(13): 2183. https://doi.org/10.3390/buildings15132183
[13] Siddique, A., Baitab, D.M., Khan, M.I., Asghar, M.A., Afzal, A., Umair, M. (2025). 3D Woven interlocking patterns with enhanced mechanical and thermophysical characteristics. Journal of Engineered Fibers and Fabrics, 20: 15589250251342852. https://doi.org/10.1177/15589250251342852
[14] Yu, Y., Xu, C., Hu, Z., Xiang, H., et al. (2024). Industrial scale Sea-Island melt-spun continuous ultrafine fibers for highly comfortable insulated aerogel felt clothing. Advanced Materials, 36(52): e2414731. https://doi.org/10.1002/adma.202414731
[15] Bhuiyan, M.A.R., Ali, A., Mohebbullah, M., Hossain, M.F., Khan, A.N., Wang, L. (2023). Recycling of cotton apparel waste and its utilization as a thermal insulation layer in high performance clothing. Fashion and Textiles, 10(1): 22. https://doi.org/10.1186/s40691-023-00342-y
[16] Fang, J.L., Du, J.X., Liu, Z.D. (2023). Correlation analysis between comfort and mechanical properties of sports fabrics. Journal of Fiber Bioengineering and Informatics, 16(2): 149-161. https://doi.org/10.3993/jfbim00201
[17] Liu, J., Jiang, S. (2023). Wearable properties of polylactic acid and thermoplastic polyurethane filaments 3D printed on polyester fabric. Journal of Industrial Textiles, 53: 15280837231166393. https://doi.org/10.1177/15280837231166393
[18] Gomes, D.A.C., de Novais Miranda, E.H., Resende, F.C., Villarruel, D.C.V., Mendes, L.M., Júnior, J.B.G. (2023). Analysis of the influence of wheat residues on gypsum composites. Innovation in Infrastructure Solutions, 8(1): 31. https://doi.org/10.1007/s41062-022-01007-3
[19] Karasawa, Y., Mizuhashi, H., Uemae, M., Yoshida, H., Kamijo, M. (2022). Comfort properties of fabrics knitted from a two-ply yarn derived from abacá and cotton. Textile Research Journal, 92(21-22): 4325-4341. https://doi.org/10.1177/00405175221102638
[20] Zou, W., Wang, Z., Li, Z., Sun, D. (2022). Thermochromic poplar that changes colour at 16–30°C. European Journal of Wood and Wood Products, 80(3): 741-748. https://doi.org/10.1007/s00107-022-01799-2
[21] Robert, U.W., Etuk, S.E., Emah, J.B., Agbasi, O.E., Iboh, U.A. (2022). Thermophysical and mechanical properties of clay-based composites developed with hydrothermally calcined waste paper ash nanomaterial for building purposes. International Journal of Thermophysics, 43(5): 74. https://doi.org/10.1007/s10765-022-02995-1
[22] Abo El-Ola, S.M., Elshakankery, M.H., Kotb, R.M. (2022). Integration of nanocomposite finishing on polyester fabric for enhanced UV protection, performance, and comfort properties. Journal of Engineered Fibers and Fabrics, 17: 15589250221119447. https://doi.org/10.1177/15589250221119447
[23] Akgül, E., Kizilkaya Aydoğan, E., Sinanoğlu, C. (2022). Investigation of different denim fabrics with fabric touch tester and sensory evaluation. Journal of Natural Fibers, 19(13): 5551-5565. https://doi.org/10.1080/15440478.2021.1881687
[24] Liu, L., Wei, L., Sun, F. (2021). Simultaneous-integrated evaluation of mechanical–thermal sensory attributes of woven fabrics in considering practical wearing states. Textile Research Journal, 91(23-24): 2872-2881. https://doi.org/10.1177/00405175211019903
[25] Vasile, S., Malengier, B., De Raeve, A., Deruyck, F. (2019). Influence of selected production parameters on the hand of mattress knitted fabrics assessed by the Fabric Touch Tester. Textile Research Journal, 89(1): 98-112. https://doi.org/10.1177/0040517517736471
[26] Nouemssi, G., Amine, B., Mbozoo, M., Djeumako, B., Valery, D., Ntamack, G. (2024). Physico-mechanical characteristics of earth bricks stabilized with cement and padouk sawdust residues. Open Journal of Applied Sciences, 14(7): 1788-1806. https://doi.org/10.4236/OJAPPS.2024.147117